A mechanistic model for oil recovery in a region of high oil droplet concentration from multiphasic fermentations

Da Costa Basto, Rita M.; Casals, Maria P.; Mudde, Robert F.; van der Wielen, Luuk A.M.; Cuellar, Maria C.

DOI
10.1016/j.cesx.2019.100033

Publication date
2019

Document Version
Final published version

Published in
Chemical Engineering Science: X

Chemical Engineering Science: X 3 (2019) 100033

Contents lists available at ScienceDirect

Chemical Engineering Science: X

journal homepage: www.elsevier.com/locate/cesx

A mechanistic model for oil recovery in a region of high oil droplet concentration from multiphasic fermentations

Rita M. Da Costa Basto [a], Maria P. Casals [a], Robert F. Mudde [b], Luuk A.M. van der Wielen [a,c,*], Maria C. Cuellar [a,1]

[a] Bioprocess Engineering, Department of Biotechnology, Delft University of Technology, Van der Maasweg 9, 2629 HZ Delft, the Netherlands
[b] Transport Phenomena, Department of Chemical Engineering, Delft University of Technology, Van der Maasweg 9, 2629 HZ Delft, the Netherlands
[c] Bernal Institute, University of Limerick, Castletroy, Limerick, Ireland

ARTICLE INFO

Article history:
Received 1 April 2019
Received in revised form 17 July 2019
Accepted 20 July 2019

Keywords:
Emulsion
Aggregation
Oil recovery
Multiphasic fermentation
Modelling

ABSTRACT

Multiphasic fermentations where an organic phase is spontaneously formed or when it is added for product removal are commonly used for production of valuable compounds. The turbulent conditions and the presence of surface-active compounds (SACs) during fermentation create a stable emulsion difficult to separate. A gas bubble/oil droplet separation method has been proposed to break such emulsion. In this paper, we propose a mathematical model to describe oil/bubble interaction in a region of high oil droplet concentration. Model validation was performed using a synthetic emulsion and an emulsion from a fermentation broth. By applying the optimal parameters predicted by the model, a 6- and 3-times oil recovery improvement was reached for the synthetic emulsion and the fermentation broth, respectively. In conclusion, the proposed mechanistic model allowed to improve oil recovery in the existing laboratory set-up, and can be used to optimize the separation and recovery method at large scale.

1. Introduction

Over the past two decades, industrial biotechnology has enabled the production of a broad range of products that form a second phase or in which solvents can be used for product extraction (Rude and Schirmer, 2009; Straathof, 2014). Examples of these products are long chain hydrocarbons, such as sesquiterpenes, which are often organic liquids at ambient conditions (Chandran et al., 2011). These products have many commercial applications as biofuels, cosmetics, pharmaceuticals, nutraceuticals and fine chemicals (Amyris, 2016; Cuellar and van der Wielen, 2015; Vickers et al., 2017). Due to their immiscibility in water and low density, their microbial production results in a complex mixture of four phases (aqueous medium, gas, organic phase composed of or containing the product and microbial cells) inside the bioreactor. We refer in this paper to the said organic phase as 'oil'.

Dispersed oil droplets rise due to buoyancy. Ideally, when the droplets rise, they coalesce with each other and form a clear, continuous oil phase that can be easily separated. During fermentation, however, surface-active-compounds (SACs) stabilize the oil droplets by decreasing the interfacial tension, increasing viscosity and inducing electrostatic repulsions (Heeres et al., 2014). Given the turbulent conditions typical of fermentation, instead of clear oil, a concentrated emulsion, also called cream, is formed. Such emulsions can also be formed when using solvents for product extraction during fermentations (Dafoe and Daugulis, 2014; Erler et al., 2003; Janssen et al., 2015).

Current processes use cost and energy intensive centrifugation steps, environmentally challenging de-emulsifiers and/or pH and temperature swings for breaking these emulsions after fermentation (Tabur and Dorin, 2012). Yet, several alternative techniques might be used to separate this oil from an emulsion during fermentation, *in situ,* without high costs, chemicals addition or harsh conditions. Some examples include dissolved air flotation (van Hee et al., 2006; Al-Shamrani et al., 2002), foam fractionation (Burghoff, 2012), gravity settling (Dolman et al., 2017), and more recently, gas enhanced oil recovery (GEOR) (Heeres et al., 2016).

During multiphasic fermentations, oil fractions and gas bubbles sizes are typically larger than the ones in systems where dissolved air flotation is applied (oil fractions below 0.1% and gas bubbles of 30–100 μm) (Rubio et al., 2002; van Hee et al., 2006). Foam fractionation has the disadvantage of low control at larger scales and low purities (Burghoff, 2012) and both dissolved air flotation and gravity settling require further downstream process to obtain a

* Corresponding author at: Bioprocess Engineering, Department of Biotechnology, Delft University of Technology, Van der Maasweg 9, 2629 HZ Delft, the Netherlands.
E-mail address: L.A.M.vanderWielen@tudelft.nl (L.A.M. van der Wielen).
[1] Current address: DSM Biotechnology Center, Delft, the Netherlands.

https://doi.org/10.1016/j.cesx.2019.100033
2590-1400/

clear oil layer (Dolman et al., 2017). Because of this, GEOR has been proposed as a suitable technique to separate oil from these type of emulsions (Cuellar and Straathof, 2018). This method uses gas bubbles to promote coalescence between emulsified oil droplets in a cream phase and create a clear oil layer without change in temperature, pH or chemical addition. Moreover, due to its mild operational conditions, it can be integrated with fermentation without hampering its performance (Pedraza-de la Cuesta et al., 2018). Previous studies from our group showed the potential of GEOR in oil recovery from hexadecane and yeast supernatant emulsions (Heeres et al., 2016), and from fermentation broth emulsions (Pedraza-de la Cuesta et al., 2018). A disadvantage of GEOR is that the interplay of the mechanisms behind the separation method is not well understood yet. This hinders oil recovery optimization and currently does not allow it to compete with conventional methods, which have been reported to result in up to 90% oil recovery from fermentation broth (Renninger, 2010; Tabur and Dorin, 2012). Heeres et al. showed that the limiting step for oil separation in an emulsion stabilized with SAC's, is the droplet coalescence after cream formation (Heeres et al., 2014). It has been showed that increasing oil fraction in the dispersed mixture did not have a large impact on oil recovery by GEOR (Heeres et al., 2016), yet there are no studies showing the impact of using gas bubbles directly in cream. Moreover, previous studies on GEOR applied to fermentation broths, showed that higher oil fractions can promote droplet coalescence and increase oil recovery (Pedraza-de la Cuesta et al., 2018).

In this paper, we propose a mathematical model that describes the interactions between gas bubbles and oil droplets in a cream in order to predict oil coalescence – and thus, oil recovery – for given emulsion and gas phase properties. Model validation is experimentally performed with a synthetic emulsion and with an emulsion from fermentation broth. Finally, the model is used to identify further improvement opportunities for the technology.

2. Model development

2.1. Mathematical model development of GEOR in a cream region

In GEOR, the gas bubbles travel under laminar conditions through a cream region which is a mixture of water and oil droplets, enabling coalescence of oil droplets onto clear oil on top (Fig. 1). Several mathematical models from literature on oil coalescence were analysed. A summary of which can be seen in Table 1.

Based on preliminary experimental studies, the aggregation model and the oil bursting model with an oil layer are the ones describing better the oil recovery by GEOR in a cream layer with oil on top. Hence, a model is proposed, integrating these two models, while preserving their main characteristics (Fig. 2). In this model, a bubble goes through the cream layer (z_{cream}) and some of the oil droplets gets attached to the hydrophobic surface of the gas bubble [A]. This event can be mathematically described by the aggregation mechanism (in food technology commonly used as flocculation). Once the gas bubble reaches the interface between the cream and the oil, a jet of cream is formed into the clear oil. The oil droplets attached to the rising bubble during aggregation are inside this cream jet [B]. With the continuous rising of the bubble, the jet gets thinner, more unstable and with oscillations. Due to the instability and the interaction between the upward hydrodynamic force created by the bubble rising and the downward force due to gravity (Ueda et al., 2011), the pressure increases and some droplets are released coalescing with the surrounding oil, described by the oil bursting mechanism [C]. During aggregation the surfactant prefers the hydrophobic/hydrophilic interface. Hence, at the time of the bursting mechanism, it is assumed that the oil attached to the bubble and further released by the jet, is not covered with surfactant and coalescence can occur (Hotrum et al, 2003). After the jet breakage, the bubble with the non-released oil droplets rises to the oil-air interface and is released to the surface [D]. The remaining cream and droplets, with a higher density than the surrounding oil, are back mixed to the cream layer [E].

To quantify the amount of oil recovered, a mass balance in the oil layer and cream layer is made. It is assumed that bubble and droplets sauter mean diameters are constant over time since preliminary works showed that coalescence between droplets/bubbles of this size was negligible (Heeres et al., 2016). In the same way, the density of both oil and cream are assumed constant, hence the model can be expressed as a volume balance.

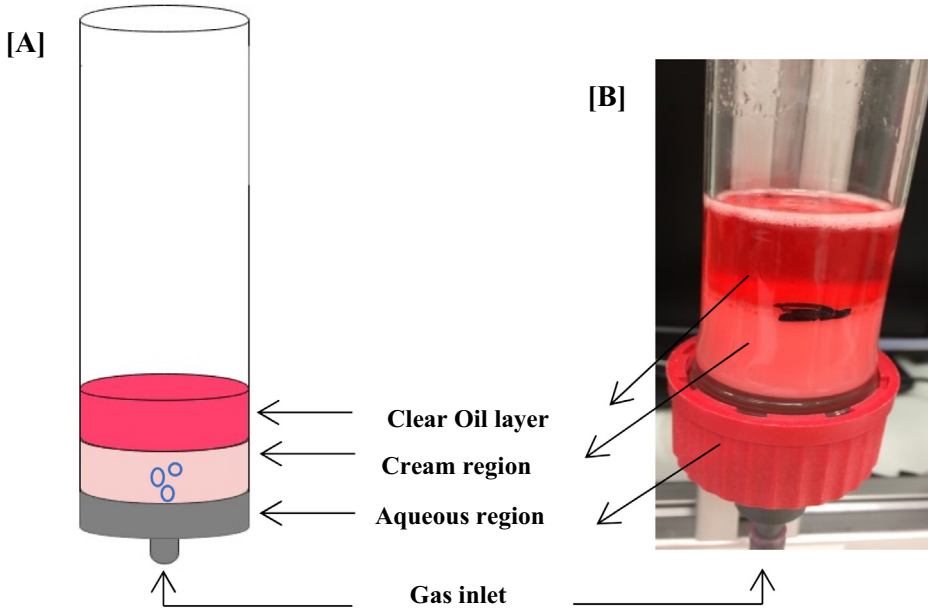

Fig. 1. Schematic drawing [A] and picture [B] of a laboratory column set-up (Column diameter (D_{col}) = 3.6 cm) with a cream region with clear oil on top.

Table 1
A summary of the different mechanisms depicted in literature that can describe oil droplets-gas bubble interactions.

Mechanisms	Description	Application studied	References
Aggregation	Attachment of oil droplets to gas bubbles and formation of an aggregate that rises to the top and promotes coalescence.	Food industry describing the attachment of fat globules to bubbles.	(Hotrum et al., 2005; Walstra, 1993, 2003)
Bursting with film layer	Droplet coalescence is promoted by the excess of surface energy from the bursting of a bubble when passing through the interface of a thin film layer and air.	Environmental, chemical and biological industries describing the burst of a bubble passing a film layer of oil.	(Feng et al., 2016; Schlichting et al., 1960; Stewart et al., 2015)
Bursting with oil layer on top	The gas bubble when passing through the interface of a dense fluid region and the oil layer, creates a column until it breaks and promote oil droplets coalescence.	Chemical industry describing the passage of a bubble through Oil-Water interface.	(Kemiha et al., 2007; Reiter and Schwerdtfeger, 1992; Singh and Bart, 2015; Uemura et al., 2010)
Flotation and Population Balance Equations	The coalescence of oil droplets in a well-mixed, two-phase system is described by several mathematical models and experimental data defining droplet coalescence and break-up, as well as rates and efficiencies.	Mineral industry and chemical industry for particle separation and multiphasic flows studies.	(Jovanović and Miljanović, 2015; Koh and Schwarz, 2008; Ralston et al., 1999; Simon et al., 2003)

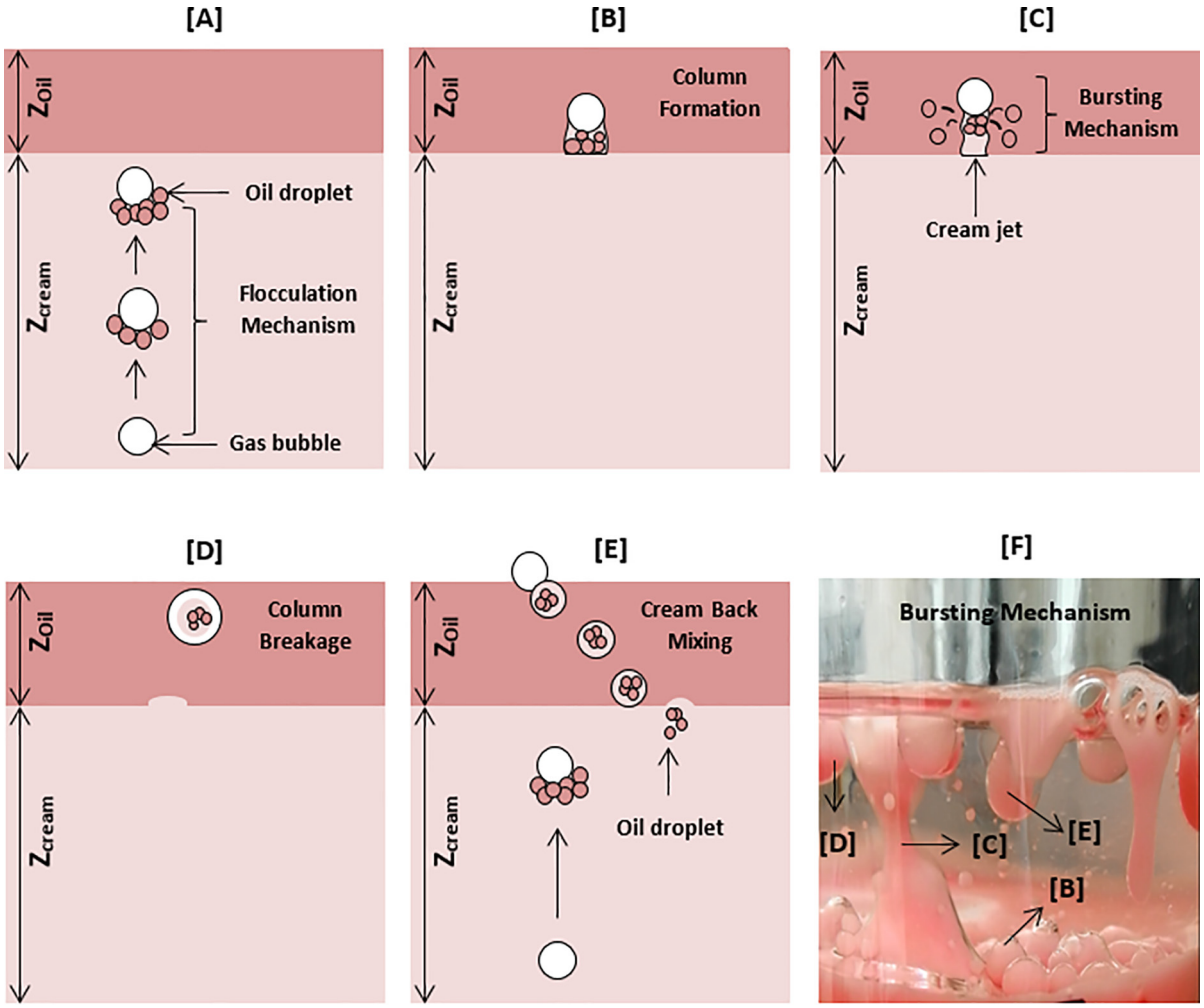

Fig. 2. Schematic representation of the mechanistic model describing oil recovery by GEOR in a cream layer with oil on top: [A] aggregation mechanism – rising of the gas bubble through the cream layer and attachment of oil droplets; [B] Cream jet formation with the oil droplets, previously attached, inside; [C] Rising of gas bubble through the oil layer and oil release due to pressure increase inside the cream jet; [D] Jet breakage and rising of gas bubble with remaining cream and oil; [E] Gas bubble release into the surface and back mixing of cream and oil droplets back to the cream. The cream merges into the cream layer and the oil droplets become available to aggregate to a gas bubble; [F] Experimental picture of the different steps [B–E] when the gas bubbles crosses the interface between the top of the cream layer and the oil layer.

The oil recovered is calculated by multiplying the rate of bubbles (Q_{Nb} in s^{-1}) by the difference of the oil attached to the bubble ($V_{oil\ aggregation}$ in m^3), and the non-coalesced oil during bursting ($V_{oil\ bursting}$ in m^3) (Eq. (1)). Q_{Nb} is given by gas inflow in the column divided by the volume of the bubble.

$$\frac{dV_{oil}}{dt} = Q_{N_b} \cdot \left[V_{oil\ \ aggregation} - V_{oil\ \ bursting}\right] \quad (1)$$

Aggregation model:

$V_{oil\ aggregation}$ is defined by the number of droplets attached to the bubble at the top of the cream layer ($N_{b\text{-}d(zcream)}$), and by the droplet volume (V_d in m^3):

$$V_{oil\ \ aggregation} = N_{b-d(zcream)} \cdot V_d \quad (2)$$

The cream height (z_{cream} in m) is reduced in time. This height is dependent on the number of droplets in the cream (N_d), the droplet volume (V_d in m^3), the cross-sectional area of the column (A_{col} in m^2) and the oil fraction in the cream (φ), which is assumed constant during the oil recovery process (Eq. (3)).

$$\mathbf{z_{cream}} = \frac{\mathbf{N_d} \cdot \mathbf{V_d}}{\mathbf{A_{col}} \cdot \varphi} \tag{3}$$

For a monodisperse emulsion, the change in N_d becomes:

$$\frac{\mathbf{dN_d} \cdot \mathbf{V_{cream}}}{\mathbf{dt}} = \left[-\mathbf{Q_{N_b}} \cdot \frac{\mathbf{V_{oil\ \ aggregation}} - \mathbf{V_{oil\ \ bursting}}}{\mathbf{V_d}}\right] \tag{4}$$

The bubble position in the cream was calculated from the bubble-droplet velocity (v_{bs}) at each time step. This velocity was obtained from a force balance on the bubble-droplets aggregate and the mass of the aggregate. In order to estimate the number of droplets attached to the bubble (N_{b_d}) while travelling through the cream layer, from z = 0 (base of the cream) to z = zcream (at the cream interface), ($\frac{dN_{b\_d}}{dt}$), the approach proposed by Hotrum et al. (2005) was used. In that approach, the attachment of droplets depends on the flow conditions (J_{dorth}) and the attachment efficiency (α):

$$\frac{\mathbf{dN_{b\_d}}}{\mathbf{dt}} = \mathbf{J_{dorth}} \cdot \alpha \tag{5}$$

At z = 0, t = 0 and $N_{b\text{-}d}$ = 0. At the conditions studied in this paper, where the system is laminar and the coalescence is induced by shear, the flow in a cream layer is considered orthokinetic, which means that the bubble attachment is promoted by the turbulence created due to velocity gradients (Eq. (5)) (Hotrum et al., 2005). The so called orthokinetic rate (J_{dorth} in 1/s) is assumed to be proportional to the volume fraction of oil (φ), the shear rate gradient (Υ in 1/s), and the number concentration of droplets in the cream (N_d) (Eq. (6)). The shear rate (Eq. (7)) is directly related with cream viscosity (ϑ_{cream}) and the gas power input (P in W), generated by the superficial gas velocity (v_{GS} in m/s) (Sánchez Pérez et al., 2006).

$$\mathbf{J_{dorth}} = \frac{4}{\pi} \cdot \varphi \cdot \gamma \cdot \boldsymbol{N_d} \tag{6}$$

$$\gamma = \left(\frac{\mathbf{P}}{\vartheta_{\mathbf{cream}} \cdot \mathbf{V_{cream}}}\right)^{\frac{1}{2}} \tag{7}$$

The attachment efficiency at orthokinetic conditions, on the other hand, was estimated following the approach by Van de Ven and Mason, considering a Hamaker constant (A_H) of 10^{-20} J, that defines the interaction between two particles and the collision radius (r_{coll}), depicted as the sum of the two particles radius (Chen et al., 1998; van de Ven and Mason, 1977). From these derivations it can be seen that the aggregation mechanism is favoured by a low droplet volume and a high shear rate gradient.

Oil bursting model:

When the bubble rises towards the oil-air interface, a cream jet increases in height (z_{jet}) until the point that it breaks (Fig. 2–[B] and [C]). According to Ueda et al. (2011), such jet breaks in three parts: the lower part, that returns to the cream region, the upper part, that gets attached to the bubble (eventually returning to the cream region) and the middle part, where part of the oil droplets coalesces into the clear oil. Hence, oil recovery due to oil bursting is calculated by the volume of the upper part of the jet formed (Fig. 3). This jet was considered as an oscillating cylinder; therefore, the volume is integrated over its length (l_b in m) (Eq. (8)). The diameter of the cream jet changes in space with an oscillating function, where A is the amplitude of the wave and y the phase. The r_{jet} was defined by the minimum radius that the cream jet could achieve.

$$\mathbf{V_{oil\ \ bursting}} = \int_0^{\mathbf{lb}} \frac{\pi}{4} \cdot \left[2 \cdot \left(\mathbf{r_{jet}} + \mathbf{A} + \mathbf{A} \cdot \mathbf{sin}\left(2 \cdot \frac{\pi}{\lambda} \cdot \mathbf{z_{jet}} + \frac{\pi}{2}\right)\right)\right]^2 \mathbf{dz_{jet}} \tag{8}$$

The length of the upper part of the cream jet (l_b) is defined by Eq. (9). This parameter depends on the bubble velocity at z_{cream} (v_b in m/s) at the cream interface, Reynolds number (Re) and Weber number (We) of the aggregate, amplitude of the cream jet (ε in m) and jet radius (r_{jet} in m) (Ueda et al., 2011).

$$\mathbf{l_b} = 2 \cdot \mathbf{r_{jet}} \cdot \ln\left(\frac{\mathbf{r_{jet}}}{\varepsilon}\right) \cdot \left(\sqrt{\mathbf{We}} + 3 \cdot \frac{\mathbf{We}}{\mathbf{Re}}\right) \tag{9}$$

$$\varepsilon = \frac{\mathbf{r_{jet}}}{\mathbf{Mo} \cdot \mathbf{C}} \tag{10}$$

The jet radius (r_{jet}) and a constant (C) were both fitted from preliminary experiments with synthetic emulsion at varying gas flows and bubble diameters (see Section 4.1). The r_{jet} is a parameter dependent on bubble diameter and should not be larger than the bubble diameter (Ueda et al., 2011). The amplitude of the cream column (ε) (Eq. (10)) was linked to the properties of the cream through the Morton number (Mo), as reported by Ghabache and Séon (2016). A sensitivity analysis was performed (Section 4.2) to understand the impact of the empirical parameters in the modelled

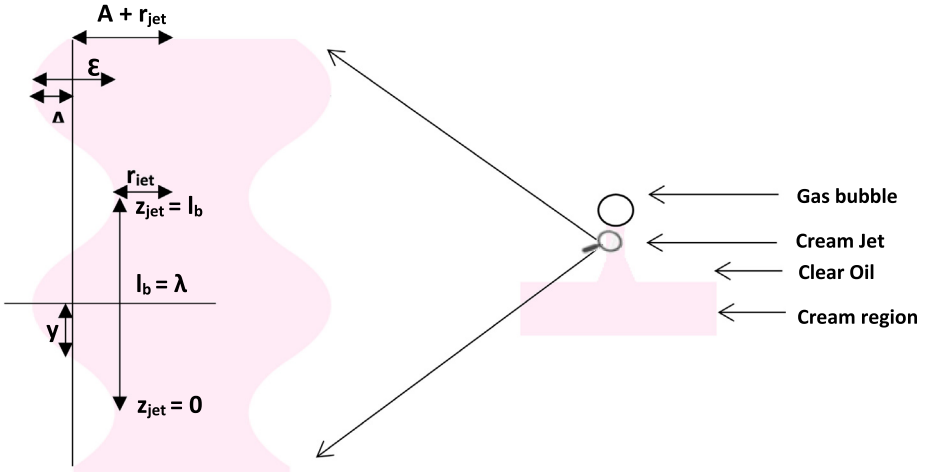

Fig. 3. Scheme of the upper part of the cream jet compared with the oscillation function adapted from Ueda et al. (2011). Where A is the wave amplitude, y the phase, λ the period, ε the amplitude of the cream jet, rjet is the radius of the cream jet and lb the length of the jet.

oil recovery. In general terms, it can be deduced from the above equations that oil bursting is favoured by a large bubble size and/or a low aggregate velocity.

2.2. Model implementation

The mathematical model described in Section 2.1 (Eqs. (1)–(10)) was implemented in MATLAB R2015b for academic users. For a given emulsion (Section 3.2) and gas properties, the model calculated the oil recovery. The bubble diameter is an input parameter dependent on the nozzle size. The input time was considered the time taken during an experimental run (3600 s). This oil recovery was normalized by the number of bubbles for comparison between different v_{GS} (Fig. 4).

3. Materials and methods

3.1. Materials

Separation experiments were performed with two mixtures: a synthetic emulsion and fermentation broth from a sesquiterpene fermentation operating with in-situ solvent extraction of the sesquiterpene product. The synthetic emulsion was prepared using MilliQ water (18.2 MΩ, Millipore systems), a non-ionic surfactant, Tween80 (Sigma Aldrich, Premium) and hexadecane (Sigma Aldrich, Reagent Plus) coloured with Oil Red O dye (Sigma Aldrich). The second phase added to the fermentation broth was dodecane (Sigma Aldrich, Reagent Grade) also coloured with Oil Red O dye.

3.2. Emulsion preparation

3.2.1. Synthetic emulsion

The synthetic emulsion was prepared by adding 1.5 L volume of MilliQ water, 0.01 mg/g of Tween80 and 0.1 v/v of coloured hexadecane to a 2 L stirred vessel with a six bladed rushton turbine (diameter of 45 mm) and two baffles (inner diameter of 120 mm) with in-situ monitoring of droplet size (see Section 3.4.1). The mixture was stirred for two hours at a rate of 1200 rpm, corresponding to a power input of 6.8 kW/m^3, and room temperature (18–20 °C).

Table 2
Fermentation conditions for the fermentation broth used during separation column experiments.

Time of harvest[1] (h)	63.0
Fermenter Volume (L)	7
Power Input (rpm)	470
Average Power Input (kW/m^3)	2.27
Cell density (g_X/kg_{broth})	25.0
Dodecane (%w/w)	9.07

[1] Being time 0 the start of the batch phase.

3.2.2. Emulsion from fermentation broth

The fermentation broth used in this work was obtained from a fermentation performed with a recombinant, sesquiterpene producing *E. coli* BL21(DE3) strain cultivated in 2 L fermenter following the protocol as described by Pedraza de la Cuesta (2019).The microorganism was cultivated aerobically at 30 °C in fed-batch mode in a medium containing glycerol as carbon source. The fermentation conditions and general composition at the time of harvest are summarised in Table 2.

3.3. Separation experiments

Separation experiments were performed either using the whole mixture prepared as described in Section 3.2 (bulk experiments) or using a concentrated mixture (cream experiments). The latter was obtained by transferring the whole mixture to a 2 L glass decanter and harvesting the concentrated oil after one hour.

Cream experiments were performed for parameter fitting and model validation. Bulk experiments were done to study the effect of bulk in oil recovery, to compare it with previous experimental data (Heeres et al., 2016) and, to understand which settings could be used to optimize oil recovery when using fermentation broth.

3.3.1. Parameter fitting experiments

For the parameter fitting, cream experiments with synthetic emulsion were executed as shown in Fig. 1 using a similar set-up and protocol as described by Heeres et al. (2016). All the experiments were performed in duplicate, originated from different mixtures. Gas sparging was generated by single orifice nozzles with varying diameters (d_{nozzle}: 0.05, 0.1, 0.3 and 1 mm). The superficial gas velocity varied between 0.05, 0.1, 0.5 and 1 cm/s. The air supply

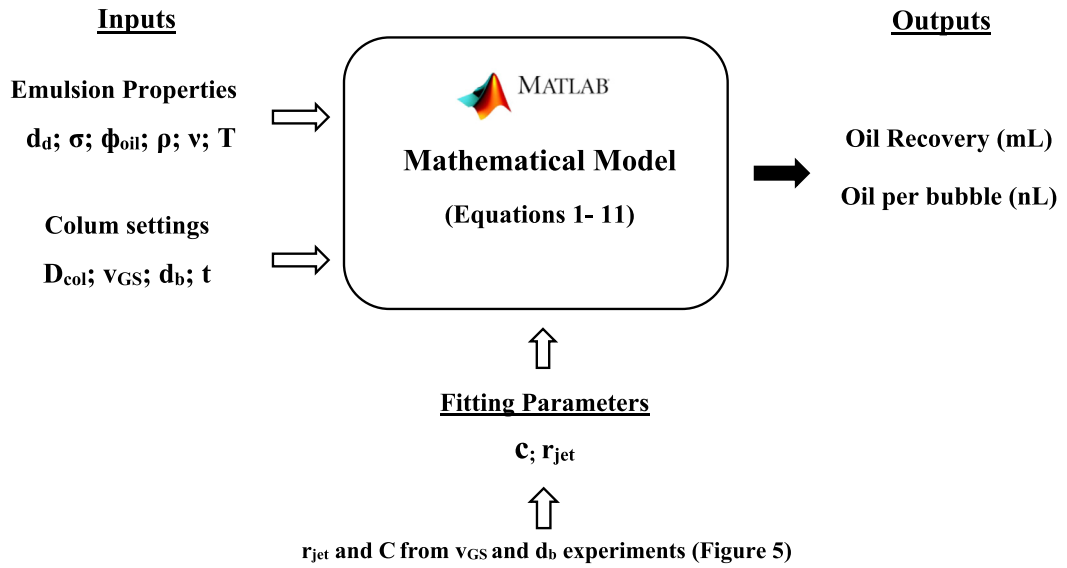

Fig. 4. Inputs, outputs and fitting parameters implemented in the mathematical model described in Section 2.1.

pressure was set at 3 bar and monitored using a manometer. An extra manometer was added between the mass flow controller and the column to detect nozzle blockage. 15 mL of the decanted aqueous solution was added to the bottom of the glass columns to account for the non-visible volume of the glass column. To the top of this liquid, 2.5 cm of cream was added. A clear oil layer, with a volume 10 times the measured bubble Sauter mean diameter (see Section 3.4.2), was set on top of it. The oil height was maintained during the experiment by removing the oil when it reached 2.4 cm oil height (corresponding to approximately 5% increase in the oil layer). After 1 h sparging, the gas flow was stopped, the mixture was let to phase-separate and the volume of clear oil recovered was determined.

3.3.2. Model validation experiments (S1 and S3)

Model validation experiments were performed with synthetic emulsions. Experiments followed the previous protocol (Section 3.3.1). An oil layer, with a volume of 5 or 10 times the measured bubble Sauter mean diameter, was set on top of the cream. The oil height was maintained during the experiment by removing the oil when it reached 2 or 2.4 cm height, respectively. Each separation experiment was performed in duplicate, originated from the same mixture. The control experiment S1, was replicated 7 times from independent mixtures and for each independent mixture, duplicates were performed (total of 14 experiments). Experiment S3, was replicated two times from independent mixtures, each performed in duplicates. Different process parameters were used for the optimization experiments and can be found in Table 3.

Cream Experiments (S2)

For the cream experiments, a single orifice nozzle with 0.3 mm diameter and superficial gas velocity of 0.2 cm/s (d_b: 0.38 cm) were set.

Bulk Experiments (S4 and S5)

Bulk experiments contained 150 mL of the whole mixture instead of the 15 mL aqueous solution. A nozzle with 0.1 mm diameter was used. Two different experiments were performed: 1 or 5 nozzle orifices and a superficial gas velocity of 0.1 cm/s (d_b: 0.23 cm) and 0.12 cm/s (d_b: 0.39 cm) were employed.

3.3.3. Experiments with emulsion from fermentation broth

When using fermentation broth, two different experiments were performed: bulk experiment (B1b and B1c), with oil set on top of the bulk phase, since there was not enough cream generated to perform all experiments, and cream experiments (B1d) with 25 mL cream and oil on top. To ensure mixture homogeneity from the reactor to the columns, the broth was first transferred to a smaller vessel which, was manually agitated before pouring into the columns. The same protocol as the previous sections (Sections 3.3, 3.3.1 and 3.3.2) was performed. The experiments were performed in duplicates originated from the same fermentation broth. The settings for the separation experiments with emulsion from fermentation broth, can be seen below (Table 4).

3.4. Analytic tools

3.4.1. Droplet size measurements

The droplet size during synthetic emulsion preparation was monitored using an optical probe (SOPAT Gmbh – detection range from 15 μm to 1000 μm) (Maaß et al., 2012). The probe was set in the emulsion preparation vessel as presented in Heeres et al. (2015). During the two hours of stirring, 1200 pictures (30 pictures every 3 min) were taken in-situ. Particle detection was obtained using the SOPAT software. To minimize the particle selection and avoid false particles detection such as gas bubbles, a threshold higher than 0.8 was set. The number of pictures taken were such that it was possible for the software to obtain at least 1 000 particles of interest. The detected particles were then analysed in the SOPAT result analyser resulting in a Sauter mean diameter of 40 ± 4 μm.

3.4.2. Bubble size measurements

The gas bubble size distributions in the separation columns were determined for all nozzles and gas flows by image analysis of a 40% ethanol solution in MilliQ water. Pictures were taken every 5 min with a digital camera (Canon 100D and a 18–55 mm lens) in a dark room. Behind the columns, a white LED (Dell, model R2412Hb, full brightness and standard colour settings) was placed. The camera was set at a height of 108 cm of the floor and a distance of 85 cm of the columns. The pictures were processed with an image analyser software (ImageJ 1.47) considering the bubbles as ellipsoids and manually marking their minimum and maximum diameters.

The Sauter mean diameter was later determined using the ellipsoid bubble volume but assuming a spherical shape of the bubble.

3.4.3. Interfacial tension measurement in synthetic emulsion

The interfacial tension (IFT) of the organic phase (hexadecane) in a continuous phase (100 mg/L of Tween80 in MilliQ water) was measured using a Drop Shape Analyser (model DSA100, Krüss, ADD country). The measurement followed the pendant drop

Table 3
Experimental oil recovery and experimental conditions and model prediction with standard deviation during separation column experiments for the control (S1) and optimization (S2, S4,) columns at lab scale (D_{col} = 3.6 cm) for a synthetic emulsion with a Sauter mean droplet sauter mean diameter of 40 μm.

	S1	S2	S3[1]	S4	S5[1]
Aqueous solution or Bulk volume (mL)	15	15	150	150	300
Cream layer height (cm)	2.5	4	2.5	2.5	–
Nozzle (mm)	0.1	0.3	0.1	0.1	0.1
#Holes	1	1	1	5	1
Oil Layer/d_b (cm)	10	5	10	5	–
Bubble Sauter mean diameter (cm)	0.23	0.38	0.23	0.39	0.23
Superficial gas velocity (cm/s)	0.1	0.2	0.1	0.12	0.1
Model Prediction					
Oil recovery (mL)	5.88	18.6	–	7.0	–
Oil recovery (%)	33	65	–	40	–
Experimental Results					
Oil recovery (mL)	5.5 ± 0.5	18.1 ± 1	3.0 ± 0	8.7 ± 0.5	3.9 ± 0.4
Oil recovery (%)	31 ± 3	64 ± 4 p-value = 0.01	17 ± 0 p-value = 0.02	49 ± 2 p-value = 0.02	13 ± 1 p-value = 0.03

[1] S3 and S5 settings were not used for model validation. Only used for oil recovery comparison.

Table 4
Oil recovery and experimental conditions during separation column experiments for the broth of a 7 L fermentation (B1) performed at a power input of 2.78 kW/m^3 (one column per condition) in a column of 3.6 cm diameter. Where B1a uses the same settings as S3 but no oil on top, B1b uses the same settings as S3, B1c uses the optimized settings from S4 experiment and B1d uses the same settings as S2 but with a 2.5 cm cream layer.

Type of mixture	B1a[1]	B1b	B1c	B1d
Volume (mL)	200	150	150	25
Nozzle (mm)	0.1	0.1	0.1	0.3
n° nozzles	1	1	5	1
Superficial gas velocity (cm/s)	0.1	0.1	0.12	0.2
Oil layer on top (cm)	no	2.2	2	1.9
Bubble diameter (cm)	0.23	0.23	0.39	0.38
Oil recovery (mL)	2.8 ± 1	4.7 ± 1	5.3 ± 1	4.8 ± 1
Oil recovery (%)	15 ± 4	35 ± 4	39 ± 4	–

[1] B1a experiment was only used for oil recovery comparison.

method, using a stainless steel J-Shaped Needle (NE71, d_{needle} = 0.487 mm, ADD supplier), where a drop of organic phase (oil phase) was submerged into a continuous phase (aqueous phase) (Science). The measurement was performed at room temperature and recorded until the IFT values of the mixture reached a plateau.

3.4.4. Oil fraction measurement in synthetic emulsion

To quantify the oil fraction in the cream, 12 mL of the cream obtained, as described in Section 3.3, were processed through a Whatman filter with a PTFE membrane of 0.45 μm pore size. The oil recovered was measured in a graduated cylinder. Two passages were necessary to achieve a clear oil. Three different set of measurements were performed. An average oil fraction of 0.7 ± 0.05 was measured.

3.4.5. Statistical analysis

The statistical significance of oil recovery yield for the different separation column experiments was evaluated by a one-tailed Student's *t*-test, assuming a heteroscedastic population for S2 and homoscedastic population for S3, S4 and S5 at a significance level of 5%.

4. Results

4.1. Parameter fitting and model validation experiments

Two parameters of the bursting model, r_{jet} and constant C, required experimental fitting. Two set of experiments were performed (see Section 3.3.1), one at constant bubble diameter (d_b = 0.23 cm) and different superficial gas velocities (v_{GS} = 0.05–1 cm/s) (Fig. 5A) and other at constant superficial gas velocity (v_{GS} = 0.1 cm/s) and different bubble diameters (d_b = 0.16–0.55 cm) (Fig. 5B). From the graphic representations of Ueda et al. (2011), it is observed that the cream jet formation (Fig. 3) is dependent on the gas bubble, hence the r_{jet} is also a function of the bubble diameter. For our system, it was found that the r_{jet} dependence on bubble diameter (both in meters) follows a power equation given by the following empirical Eq. (11).

$$\mathbf{r_{jet}} = 1.2\times10^{-6}.(\mathbf{d_b})^{-1.22} \quad (11)$$

The amplitude of the cream jet is linked with the cream properties and the jet radius. However, their relation is also no yet reported in literature. For that reason, a constant, C, with a value of 9.2×10^7, needed to be experimentally fitted with the experimental data. Although these two parameters can be related to each other as one constant (see Eq. (10)), the two were fitted separately to be sure that r_{jet} would be consistent with the cream jet geometry and would not be larger than the bubble diameter.

The y-axis represent the oil recovery normalized per bubble. For both experiments it is observed that lower superficial gas velocities and larger bubble diameters resulted in higher oil recovery per bubble. However, the maximal experimental oil recovery achieved was 36%, for a superficial gas velocity of 0.1 cm/s and a bubble diameter of 0.23 cm, calculated as the percentage of oil recovered relative to the total oil initially present in the cream. Both Fig. 5A and B are at the same conditions (db = 0.23 cm and vGS = 0.1 cm/s) have given an equal oil recovery per bubble. The increase of bubble diameter will decrease the number of bubbles in the system and the oil recovery per bubble will increase. For larger bubble diameters, this increase is exponential and oil recovery per bubble becomes order of magnitudes higher. For smaller bubble

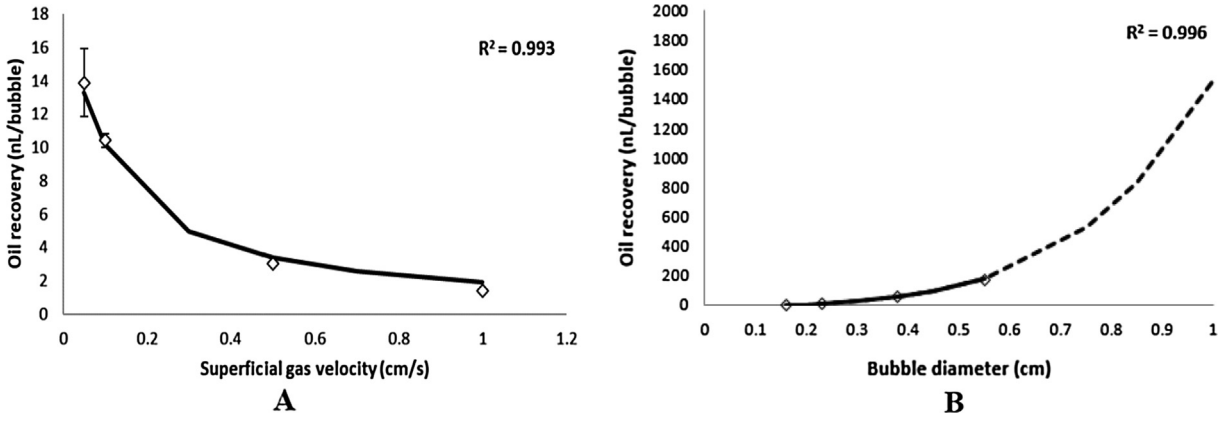

Fig. 5. Oil recovery normalized per number of bubbles experiments for (A) parameter fitting at different v_{Gs} and d_b = 0.23 cm; (B) parameter fitting at different bubble Sauter mean diameters and v_{Gs} = 0.1 cm/s. For d_b smaller than r_{jet} it was assumed the recovery was 0. Solid line represents the model fitting for (A) 4 different v_{Gs} and for (B) 4 different d_b. White markers represent the experimental data. Dash line represents the model extrapolation without experimental fitting.

diameters, the oil recovery per bubble is in the same order of magnitude as the oil recovery shown by Fig. 5A.

The fitting parameters were then used to predict the best parameters (v_{GS}, d_b, D_{col}) required to reach an oil recovery higher than 90%. Two different systems were evaluated for the lab scale set-up (D_{col} = 3.6 cm): a cream layer with clear oil on top, and a bulk phase with a cream layer and oil on top. A range of 0.1–1 cm for bubble diameter and superficial gas velocities was simulated (Fig. 6). For bubble diameters lower than 0.2 cm the oil recovery was considered 0 since the r_{jet} was smaller than the bubble diameter. Other parameters, such as droplet size, were not implemented to predict oil recovery since they only have a negligible influence in the model estimations (see Section 4.2).

An oil recovery percentage of 74% and 84% was observed for d_b = 1 cm and v_{GS} = 0.1 cm/s (Fig. 6) when using a cream layer of 2.5 cm and 4 cm (results not shown), respectively. For bubble diameters between 0.6 and 1 cm, the model could not be experimentally validated and the empirical correlations might not be valid for this range of bubble diameters. In addition, a parameter that was not taken into account for model development (Section 2.1) was the foam formation at higher v_{GS} and larger d_b. Based on experimental results and to avoid errors in oil recovery optimization, a foam region was identified at v_{GS} higher than 0.5 cm/s and d_b larger than 0.6 cm. Taking this into account, at this scale a maximal oil recovery percentage of only 59% and 74% can be predicted for a cream layer of 2.5 cm and 4 cm, respectively.

For both cream heights, the same trend is perceived. Higher superficial gas velocities and smaller bubble diameters lead to lower oil recovery (as shown in Fig. 5). Moreover, the model showed that oil recovery has the tendency to become constant regardless the increase of superficial gas velocities or bubble size (e.g.: d_b = 0.6 cm and v_{GS} = 0.6 cm/s). For a constant superficial gas velocity and increasing bubble diameter the number of bubbles in the system decreases, and so does the oil recovery. On the other hand, if the superficial gas velocity increases, the number of bubbles in the system increases and there is a decrease in oil recovery efficiency per bubble (Fig. 5). Hence, to reach higher oil recovery, there must be a trade-off between number of bubbles in the system and superficial gas velocities. This can be confirmed by the fact that at higher superficial gas velocities and lower bubble diameters (d_b = 0.3 cm and v_{GS} = 0.6 cm/s) the oil recovery become equal or even higher than for bubble diameters of 0.4 cm.

This mathematical model is validated on laboratory scale. For testing the impact of oil recovery in larger diameters, a cream volume between 0.5 and 2.5 L would be necessary per experiment, requiring a reactor of at least 10 L per column experiment to obtain the emulsions. Given this perspective, a model-based analysis was implemented to assess the impact of column diameter on the predicted oil recovery (Fig. 7). It can be seen that recovery larger than 90% can be achieved for column diameters 5x larger than the laboratory scale column (D_{col} = 3.6 cm). By changing the column diameters, the rate of bubbles (Q_{NB}) will increase, enhancing the recovery of oil. Interestingly, by expanding the column diameters, the effect of changing superficial gas velocity and bubble diameters, in the range studied, becomes negligible, which allows a more robust operation at larger scales.

4.2. Sensitivity analysis

During the course of model development, three major assumptions were made: (a) bubble size was assumed equal to that measured in a 40% ethanol solution; (b) constant droplet size throughout the experiment (40 μm); and (c) use of empirical parameters - C and r_{jet}. Moreover, physical parameters, such as, interfacial tension and oil viscosity are known for the mimic emulsion. However, if a different emulsion is used where these parameters are not known or are not easily determined (e.g.: fermentation broth), then to understand their effect in oil recovery is of utmost importance. Therefore, sensitivity analysis was performed to these parameters to evaluate their effect in the oil recovery prediction by the model. The r_{jet} parameter was not studied by sensitivity analysis since his value is given by a power equation (Eq. (11)) which is dependent on the bubble diameter. In this context, the above-mentioned parameters were varied. The constant C was increased and decreased by one order of magnitude to understand if there was any impact on the model results. The oil viscosity extremes were defined by the model boundaries. For oil viscosities outside this range, the model does not work. The interfacial tension and droplet sauter mean diameter were varied taking into account the range of values of a stable emulsions (low

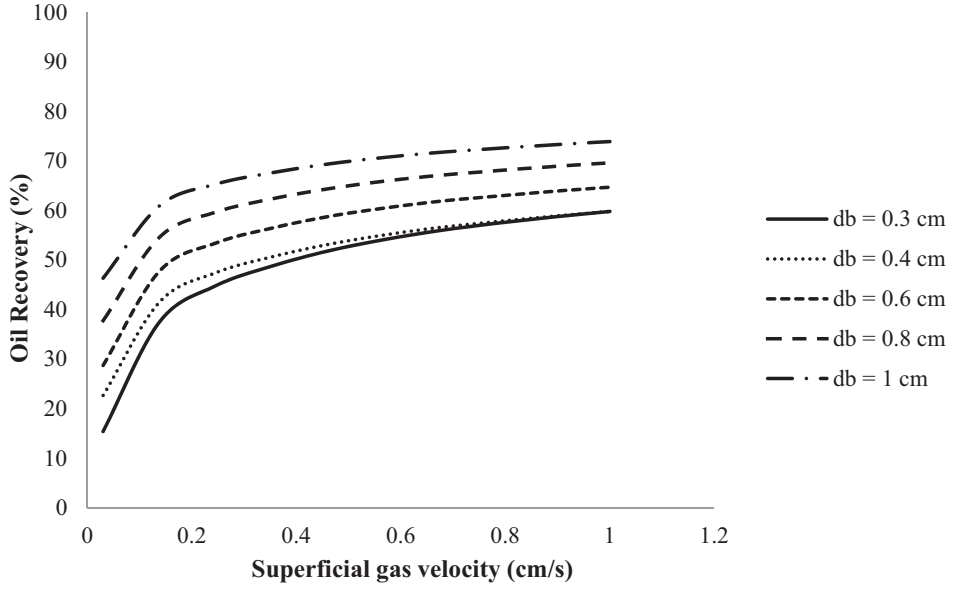

Fig. 6. Total oil recovery (%) predicted by the model as a function of gas velocities and bubble diameter for a synthetic emulsion cream layer of 2.5 cm and D_{col} 3.6 cm. For d_b lower than 0.2 cm it was assumed that the oil recovery was zero since r_{jet} was smaller than d_b.

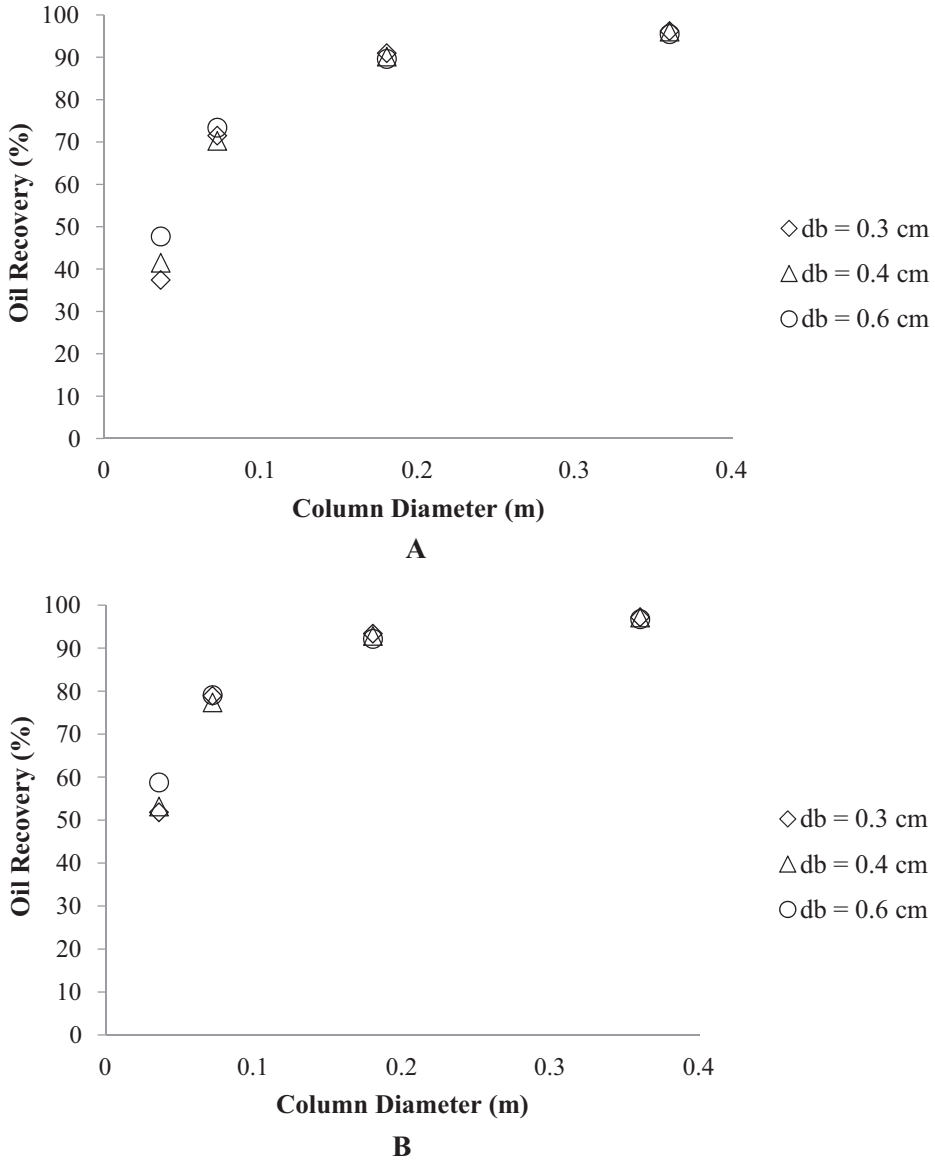

Fig. 7. Estimated total oil recovery (%) predicted by the model for an increase of 2×, 5× and 10× of the lab scale column diameter (D_{col} = 3.6 cm) for different bubble diameters and two different superficial gas velocities: (A) v_{GS}: 0.14 cm/s v_{GS}; (B) v_{GS}: 0.46 cm/s for a synthetic emulsion cream layer of 2.5 cm.

extreme) and a weaker emulsion (higher extreme). The oil fraction was varied between the minimum and maximum values that can be found in a multiphasic fermentation. The effect of these parameters on the model results was analysed (Fig. 8). For the Sauter mean bubble diameter its impact on oil recovery could already been seen in Section 4.1. Moreover, by changing ±0.1 cm, using a randomized method following a Gaussian distribution, the change in bubble diameter showed a standard deviation of 0.6 mL, which follows inside the experimental error.

It is observed that the oil recovery is highly influenced by the change in oil fraction and interfacial tension. Where higher oil recovery is achieved for higher oil fraction, systems with higher interfacial tension (35 mN/m) and lower oil viscosity (1.5×10^{-3} Pa s). This shows that for each emulsion, these parameters should be always quantified previously to model predictions. Moreover, for a new emulsion a new r_{jet} equation should be previously fitted. Although this might seem counterintuitive, the parameter with less influence in the oil recovery is the droplet sauter mean diameter.

The same parameters were changed for higher column diameters. Recovery lower than 90% were found for oil fraction below 0.3, viscosity lower than 1.5×10^{-3} Pa s and droplet sauter mean diameter higher than 60 μm (results not shown).

4.3. Experiments with synthetic emulsion results

4.3.1. Cream and bulk experiments

The oil recovery percentage was measured experimentally for a synthetic emulsion using a 2.5 cm cream layer, 150 mL of bulk phase, and a fermentation broth emulsion. The settings chosen were based on the predicted model results. When comparing the experimental oil recovery with the model predictions, it is clear that similar results were achieved for S2 and S4 (Table 3). In addition, oil recovery were larger for S2, which used a 4 cm cream layer and bubble diameter of 0.38 cm, in contrast with the standard column (S1). Comparing S4 with S3 and S5 (bulk experiments), the oil recovery was doubled. However, higher oil recovery could not be reached, because none of the current

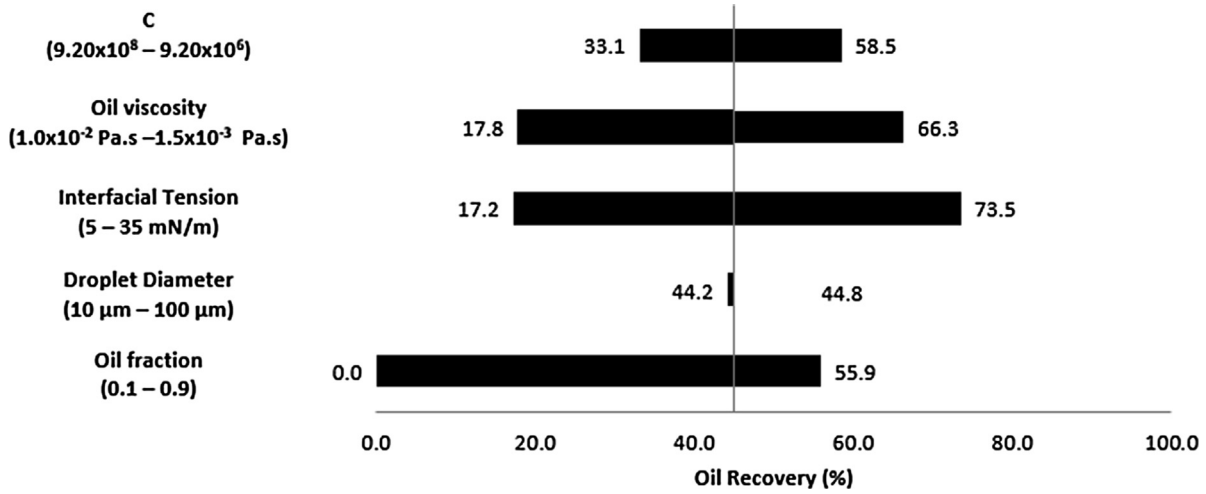

Fig. 8. Sensitivity analysis of the percentage of oil recovery for a common range of model parameters for a cream layer of 2.5 cm, D_{col} of 3.6 cm, d_b of 0.38 cm and v_{GS} of 0.2 cm/s.

nozzles promote an increase in bubble diameter as estimated by the model (Section 4.1).

4.4. Fermentation broth experiments

To assess whether the mechanisms taking place in the synthetic emulsion are comparable to those in a fermentation broth, experiments were performed using the emulsion described in Section 3.2.2. The experimental parameters, and the respective oil recovery, can be found in Table 4. The oil recovery for this specific case could not be predicted by the model, since for this type of system, the relevant parameters (such as interfacial tension, viscosity, density, droplet size and fraction of the oil in the cream) could not be measured. Four different experiments were performed: B1a, B1b and B1c – with oil on top; and B1d – only with cream and oil on top. Although the oil recovery is still low, B1b, B1c and B1d show an increase of 100% in comparison to B1a, suggesting that the two mechanisms described above are also present on a fermentation broth emulsion. The percentage of oil recovery for experiment B1d, could not be attained, since the oil fraction in the cream is not known.

5. Discussion

5.1. Improving oil recovery by scale-up

A mathematical model based on two different mechanisms, aggregation and oil bursting, was proposed in order to explain the gas bubble interaction with oil droplets in a cream layer with oil on top. A systematic approach was taken to validate the model, using a synthetic emulsion with exactly the same characteristics throughout the whole research. The normalized oil recovery, predicted by the model, was shown to fit the experimental results at varying superficial gas velocities and gas bubble Sauter mean diameters (Fig. 5). The model predicted 74% oil recovery for a db = 0.6 cm and vGS = 0.46 cm/s. Yet, the experimental results at laboratory scale showed that oil recovery higher than 64% could not be achieved, since the optimal settings predicted by the model could not be reached with the current equipment. Still, it is observed that oil recovery higher than 90% could not be reached at laboratory scale. Regardless, it can be seen that an increase in the column diameter is beneficial for enhancing oil recovery. By enlarging the column diameter, at constant superficial gas velocity, the flow rate in the system will increase, as well as the number of bubbles in the system. Because more bubbles are being fed into the system, more oil is recovered. This benefit with scale increase was also predicted by Pedraza-de la Cuesta et al. (2018), which discussed that an increase in the residence time in the column (e.g.: by increasing the column volume) could lead to higher oil recovery.

5.2. Parameter effect in oil recovery

Sensitivity analysis shows that, in the range studied, droplet sauter mean diameter and C would not have an impact on the oil recovery expected by the model. Oil viscosity has a bigger impact in oil recovery than the previous parameters. When using higher oil viscosities, it was observed that recovery was hindered. This is expected since with higher viscosity the drag force during the aggregation mechanism increases. Additionally, the Morton number in the bursting mechanism increases by the power four (Ghabache and Séon, 2016) hence the amplitude of the cream jet (Eq. (10)) is reduced in such a way that there are almost no oscillations thus, the oil is trapped inside the jet. Therefore, lower viscosities promote oil recovery in a cream layer with oil on top.

The other two parameters that have a bigger influence in oil recovery are interfacial tension and oil fraction. If the oil fraction in the cream is lower (i.e. for a different emulsion type), a decrease in the oil recovery can be expected. By decreasing the oil fraction, the amount of oil in the system will reduce and the properties of the emulsion will change. This will have an impact not only on the aggregation mechanism but also on the formation of cream jet during the bursting mechanism leading to smaller oil recovery. Despite that, with increased oil fraction the oil recovery is not much higher than the base case. Increasing the oil fraction will increase the number of droplets attached to the bubble hence, the bubble velocity will decrease due to the weight increase and consequently, hamper the bursting mechanism and hinder oil recovery.

The change in interfacial tension has a similar effect in oil recovery as the one of viscosity. For lower values of interfacial tension, there is an increase in the Weber number, increasing the length of the cream jet (Eq. (9)) and hindering oil recovery. Moreover, the impact of Morton number (Ghabache and Séon, 2016) is larger and, by decreasing the interfacial tension, the Morton number increases, and as previously described, the cream jet amplitude decreases. Thus, higher interfacial tensions result in higher oil recovery.

Droplet size show to have only a small influence in oil recovery. Nevertheless, previous experiments shown that droplet size also have an impact on the creaming behaviour of the emulsion. On one hand, for larger droplets sizes (100 μm), emulsions cream faster and oil is better recovered with GEOR (Heeres et al., 2016). On the other hand, smaller droplets size (10 μm) can take much more time to cream or not even cream (Pedraza-de la Cuesta et al., 2018), reducing the oil fraction in the system and hampering the aggregation mechanism.

Moreover, one has to consider that for lower r_{jet} values, present for larger bubble diameters, there will be an increase of pressure inside the cream jet, which leads to higher amount of oil released hence, larger oil recovery, as observed in Fig. 5B. For higher r_{jet} values, a thicker jet is formed and more oil is kept inside and further back mixed to the cream (see Fig. 2[D] and [E]). This fitting parameter is highly dependent on the emulsion properties and bubble diameter, and is not a measurable or tuneable parameter. Therefore, if the model is used on a different type of emulsion, to achieve reliable results, it is necessary to fit once more this parameter against new experimental data.

5.3. Can aggregation and oil bursting mechanisms improve oil recovery in synthetic emulsions?

The experimental results for the synthetic emulsion S1, S2 and S4 show that the model could predict quite well the oil recovery obtained by GEOR. This confirms that the model describes well the recovery of oil from a synthetic emulsion. Comparing the recovery between the standard column (S1) and the column using optimal settings from the model (S2), an increase in oil recovery was observed. For the bulk experiments (S3 and S4), the experiment with larger bubble diameter (S4) showed a 100% increase in recovery in relation to S3. Nonetheless, when comparing bulk experiments with cream experiments, lower recovery were achieved. The current results are consistent with published data (Heeres et al., 2016), where Heeres et al. concluded that bigger bubbles and lower velocities would lead to higher oil recovery. Moreover, the authors stated that in zones with increased oil fraction, oil recovery was increased. The reported oil recovery for a supernatant emulsion was 66% at the same settings as S2, which are in the same range of values as the ones reported in this paper.

5.4. Are the aggregation and oil bursting mechanisms also present in fermentation broth?

To understand if the same mechanisms described before (Section 2) are present during oil recovery from fermentation broth emulsion, both systems were compared. For fermentation broth there was no data available of important empirical parameters such as droplet size or oil fraction. Moreover, there was no possibility of fitting the r_{jet} parameter due to lack of reproducible material. Hence, the same optimal settings as for the synthetic emulsion (S4), were used (B1c). Based the sensitivity analysis results and assuming that the fermentation broth has lower droplet sizes (slower creaming) and lower oil fractions than in the mimic emulsion, one would expect that the oil recovery would be similar or lower. By comparing the oil recovery obtained by the column B1a, with no cream or oil on top, and column B1b, with oil on top, and B1d with only cream and oil on top, it is seen that there is an improvement in oil recovery for the last columns. This shows, that the aggregation and bursting mechanism, also have an impact when using fermentation broth. The results shown by Pedraza-de la Cuesta et al., also support the existence of the two mechanisms described in this paper, since for experiments with higher oil hold-up in the top of the column, there was a higher degree of coalescence and higher oil recovery (Pedraza-de la Cuesta et al., 2018). Additionally, for the column experiment B1c, the recovery obtained was similar to the one of the synthetic emulsion column experiment at the exact same conditions. This suggests that oil recovery using GEOR in fermentation broth can be described by the same mechanisms for both mixtures. Nevertheless, large oil recovery could not be reached. Further studies, on emulsion properties, oil fraction and r_{jet}, would allow a better use of the present mathematical model to decide on the optimal parameters for achieving larger oil recovery.

6. Conclusions

A mathematical model describing oil coalescence when a gas bubble is in contact with a region of high oil droplet concentration, has been presented. This model was successfully validated with a synthetic emulsion stabilised by Tween80 and was used to improve oil recovery at laboratory scale. Overall, oil recovery is governed by the aggregation mechanism, and interfacial tension, oil fraction, and oil viscosity revealed to be the parameters with higher impact in the recovery. Owing to the lack of measurable experimental parameters, the model could not be applied for fermentation broth, but provided valuable insight for parameter optimization. When using these parameters, oil recovery was enhanced by 50% over the base case for the columns with oil on top, demonstrating the significant impact of aggregation and bursting mechanisms. The model suggests that oil recovery above 90% could be achieved by increasing the surface area to volume ration of the recovery setup. Yet, relevant parameters such as viscosity, interfacial tension, oil fraction in cream and bubble diameter should be studied and optimized during fermentation to achieve higher oil recovery. In general, the results of this research shed new light on the mechanisms occurring during oil separation by gas-enhanced oil recovery and on the parameters, such as column design and fermentation broth properties, that can be adjusted to optimize the separation and recovery methods at large scale and help to reduce costs in production processes.

Declaration of Competing Interest

Since summer 2018, Prof. Luuk van der Wielen and Dr. Maria Cuellar are (indirect and minority) shareholders in DAB BV, following the TU Delft regulations for staff inventors of intellectual property.

Acknowledgements

This work was carried out within the BE-Basic R&D Program, which was granted a FES subsidy from the Dutch Ministry of Economic affairs. The authors would like to thank Dr. Christian Picioreanu for his contribution in implementing the model in Matlab. To Carla Prat for performing the fermentations and Marcelo Silva and Joana Carvalho Pereira for providing a critical discussion of this work.

Appendix A. Supplementary material

Supplementary data to this article can be found online at https://doi.org/10.1016/j.cesx.2019.100033.

References

Al-Shamrani, A.A., James, A., Xiao, H., 2002. Destabilisation of oil-water emulsions and separation by dissolved air flotation. Water Res. 36, 1503–1512.
Amyris, 2016. <https://amyris.com/innovation/biofene/>.
Burghoff, B., 2012. Foam fractionation applications. J. Biotechnol. 161, 126–137.
Chandran, S.S., Kealey, J.T., Reeves, C.D., 2011. Microbial production of isoprenoids. Proc. Biochem. 46. 8-8.

Chen, L., Serad, G., Carbonell, R., 1998. Effect of mixing conditions on flocculation kinetics of wastewaters containing proteins and other biological compounds using fibrous materials and polyelectrolytes. Braz. J. Chem. Eng. 15, 358–368.
Cuellar, M.C., Straathof, A.J.J., 2018. Improving fermentation by product removal, intensification of biobased processes. Royal Soc. Chem., 86–108 Chapter 4.
Cuellar, M.C., van der Wielen, L.A.M., 2015. Recent advances in the microbial production and recovery of apolar molecules. Curr. Opin. Biotechnol. 33, 39–45.
Dafoe, J.T., Daugulis, A.J., 2014. In situ product removal in fermentation systems: improved process performance and rational extractant selection. Biotechnol. Lett. 36, 443–460.
Dolman, B.M., Kaisermann, C., Martin, P.J., Winterburn, J.B., 2017. Integrated sophorolipid production and gravity separation. Process Biochem. 54, 162–171.
Erler, S., Nienow, A., Pacek, A., 2003. Oil/water and pre-emulsified oil/water (PIT) dispersions in a stirred vessel: Implications for fermentations. Biotechnol. Bioeng. 82, 543–551.
Feng, J., Muradoglu, M., Kim, H., Ault, J.T., Stone, H.A., 2016. Dynamics of a bubble bouncing at a liquid/liquid/gas interface. J. Fluid Mech. 807, 324–352.
Ghabache, E., Séon, T., 2016. Size of the top jet drop produced by bubble bursting. Phys. Rev. Fluids 1, 051901.
Heeres, A.S., Heijnen, J.J., van der Wielen, L.A.M., Cuellar, M.C., 2016. Gas bubble induced oil recovery from emulsions stabilised by yeast components. Chem. Eng. Sci. 145, 31–44.
Heeres, A.S., Picone, C.S.F., van der Wielen, L.A.M., Cunha, R.L., Cuellar, M.C., 2014. Microbial advanced biofuels production: overcoming emulsification challenges for large-scale operation. Trends Biotechnol. 32, 221–229.
Heeres, A.S., Schroen, K., Heijnen, J.J., van der Wielen, L.A.M., Cuellar, M.C., 2015. Fermentation broth components influence droplet coalescence and hinder advanced biofuel recovery during fermentation. Biotechnol J 10, 1206–1215.
Hotrum, N.E., Cohen Stuart, M.A., van Vliet, T., van Aken, G.A., 2003. Flow and fracture phenomena in adsorbed protein layers at the air/water interface in connection with spreading oil droplets. Langmuir 19, 10210–10216.
Hotrum, N.E., Stuart, M.A.C., Vliet, T.V., Avino, S.F., van Aken, G.A., 2005. Elucidating the relationship between the spreading coefficient, surface-mediated partial coalescence and the whipping time of artificial cream. Colloids Surf., A 260, 71–78.
Janssen, A.C.J.M., Kierkels, J.G.T., Lentzen, G.F., 2015. Two-phase fermentation process for the production of an organic compound WO 2015002528 A1 2015. Isobionics B.V.
Jovanović, I., Miljanović, I., 2015. Modelling Of Flotation Processes By Classical Mathematical Methods – A Review.
Kemiha, M., Olmos, E., Fei, W., Poncin, S., Li, H.Z., 2007. Passage of a gas bubble through a liquid−liquid interface. Ind. Eng. Chem. Res. 46, 6099–6104.
Koh, P.T.L., Schwarz, M.P., 2008. Modelling attachment rates of multi-sized bubbles with particles in a flotation cell. Miner. Eng. 21, 989–993.
Maaß, S., Rojahn, J., Hänsch, R., Kraume, M., 2012. Automated drop detection using image analysis for online particle size monitoring in multiphase systems. Comput. Chem. Eng. 45, 27–37.
Pedraza-de la Cuesta, S., Keijzers, L., van der Wielen, L.A.M., Cuellar, M.C., 2018. Integration of Gas Enhanced Oil Recovery in multiphasic fermentations for the microbial production of fuels and chemicals. Chem. Biotechnol. J.
Pedraza de la Cuesta, S., 2019. Product Emulsification in multiphase fermentations - the unspoken challenge in microbial production of sesquiterpenes, in Biotechnology. 2019, Delft University of Technology: Delft Library.
Ralston, J., Fornasiero, D., Hayes, R., 1999. Bubble–particle attachment and detachment in flotation. Int. J. Miner. Process. 56, 133–164.
Reiter, G., Schwerdtfeger, K., 1992. Characteristics of entrainment at liquid/liquid interfaces due to rising bubbles. ISIJ Int. 32, 57–65.
Renninger, N., 2010. Scale-up and Mobilization of Renewable Diesel and Chemical Production from Farnesene using US-based Fermentable Sugar Feedstocks. In: Review, D.I.B. (Ed.).
Rubio, J., Souza, M.L., Smith, R.W., 2002. Overview of flotation as a wastewater treatment technique. Miner. Eng. 15, 139–155.
Rude, M.A., Schirmer, A., 2009. New microbial fuels: a biotech perspective. Curr. Opin. Microbiol. 12, 274–281.
Sánchez Pérez, J.A., Rodríguez Porcel, E.M., Casas López, J.L., Fernández Sevilla, J.M., Chisti, Y., 2006. Shear rate in stirred tank and bubble column bioreactors. Chem. Eng. J. 124, 1–5.
Schlichting, H., Gersten, K., Krause, E., Oertel, H., Mayes, K., 1960. Boundary-layer theory. Springer. Science, K.A.y.s., Pendant Drop.
Simon, M., Schmidt, S.A., Bart, H.J., 2003. The droplet population balance model – estimation of breakage and coalescence. Chem. Eng. Technol. 26, 745–750.
Singh, K.K., Bart, H.-J., 2015. Passage of a Single Bubble through a Liquid-Liquid Interface. Ind. Eng. Chem. Res. 54, 9478–9493.
Stewart, Peter S., Feng, J., Kimpton, Laura S., Griffiths, Ian M., Stone, Howard A., 2015. Stability of a bi-layer free film: simultaneous or individual rupture events? J. Fluid Mech. 777, 27–49.
Straathof, A.J.J., 2014. Transformation of biomass into commodity chemicals using enzymes or cells. Chem. Rev. 114, 1871–1908.
Tabur, P., Dorin, G., 2012. Method for purifying bio-organic compounds from fermentation broth containing surfactants by temperature-induced phase inversion. In: Amyris (Ed.). Amyris Inc., US.
Ueda, Y., Kochi, N., Uemura, T., Ishii, T., Iguchi, M., 2011. Numerical observation of flow field around the water column behind a rising bubble through an oil/water interface. ISIJ Int. 51, 1940–1942.
Uemura, T., Ueda, Y., Iguchi, M., 2010. Ripples on a rising bubble through an immiscible two-liquid interface generate numerous micro droplets. EPL (Europhys. Lett.) 92, 34004.
van de Ven, T.G.M., Mason, S.G., 1977. The microrheology of colloidal dispersions VII. Orthokinetic doublet formation of spheres. Colloid Polym. Sci. 255, 468–479.
van Hee, P., Elumbaring, A.C.M.R., van der Lans, R.G.J.M., Van der Wielen, L.A.M., 2006. Selective recovery of polyhydroxyalkanoate inclusion bodies from fermentation broth by dissolved-air flotation. J. Colloid Interface Sci. 297, 595–606.
Vickers, C.E., Williams, T.C., Peng, B., Cherry, J., 2017. Recent advances in synthetic biology for engineering isoprenoid production in yeast. Curr. Opin. Chem. Biol. 40, 47–56.
Walstra, P., 1993. Principles of emulsion formation. Chem. Eng. Sci. 48, 333–349.
Walstra, P., 2003. Physical Chemistry of Foods. Dekker.